

# Design and experimental research of a high-precision wavelength controller for tunable fiber Fabry-Perot filters\*

QI Hai-bing (齐海兵)<sup>1,2\*\*</sup>, WEI Shu-hua (魏书华)<sup>2</sup>, and CHEN Wei (陈韡)<sup>2</sup>

1. Hubei Polytechnic University, Huangshi 435003, China

2. Wuhan National Laboratory for Optoelectronics, School of Optoelectronic Science and Engineering, Huazhong University of Science and Technology, Wuhan 430074, China

(Received 12 October 2012)

©Tianjin University of Technology and Springer-Verlag Berlin Heidelberg 2013

A high-precision wavelength controller is presented in this paper. It is necessary to find out the difference between the central wavelength of a tunable fiber Fabry-Perot (FFP) filter and that of the input laser, while the wavelength controller operates at the states of wavelength-scanning and wavelength-locking modes. Firstly, a dynamic simulation model of tunable FFP filter is established, and the dynamic characteristic of tunable FFP filter modulated by an alternating current (AC) signal is simulated. Then the measuring time at wavelength-scanning mode compared with the theory time is discussed, and this time difference shows the difference between the central wavelength of a tunable FFP filter and that of the input laser. At last, the effects on wavelength-locking precision of time delays, including the time delay of opened-loop circuit, the time constant of the closed-loop circuit and the intrinsic hysteresis of piezoelectric (PZT) element, are analyzed. A wavelength controller of tunable FFP filter is designed and prepared. The experimental results at wavelength-locking mode show that a high locking precision is obtained.

**Document code:** A **Article ID:** 1673-1905(2013)02-0101-4

**DOI** 10.1007/s11801-013-1065-3

Tunable fiber Fabry-Perot (FFP) filters driven by piezoelectric (PZT) element are critical components in optical communication applications, such as high-speed optical packet switching, wavelength demodulating, and phase-to-intensity modulation conversion. Also significant improvement in radio-over-fiber (RoF) links can be achieved by utilizing tunable FFP filters in such systems<sup>[1-3]</sup>. When it is modulated with an alternating current (AC) signal<sup>[4,5]</sup>, the tunable FFP filter can operate at either wavelength scanning mode or locking mode with the heterodyne detection technique. A precise controller for FFP is crucial in order to provide fast and stable alignment between the center wavelength of the filter and that of the laser<sup>[6-12]</sup>. However, the time delay of the opened-loop circuit, the time constant of the closed-loop system and the hysteresis of PZT element all reduce the precisions of wavelength scanning and wavelength locking<sup>[13,14]</sup>.

In this paper, a dynamic model of tunable FFP filter is established, and the dynamic characteristic of the FFP filter modulated by an AC signal is studied by this model. Then a method to make sure the real wavelength center of FFP filter is presented, which utilizes the difference between the theory time and the measuring time of the output signal. The effect of the time delay induced by

external circuit and PZT element is also considered. At last, a wavelength controller is designed, and experimental results show that it can provide high precision control.

When a small AC signal of  $V_c \sin(\omega_c t)$  is applied to a tunable FFP filter, it causes a periodical dither of the cavity length. For a beam of single-frequency laser with intensity  $I_0$  input into the filter, the signal detected by a photodetector (PD) at the output of the filter can be expressed as<sup>[15]</sup>

$$V_D = KI_0 / [1 + 4(\alpha + \beta \sin(\omega_c t))^2], \quad (1)$$

$$\alpha = (\omega - \omega_q) / \Delta\omega, \quad \beta = \rho / \Delta\omega, \quad (2)$$

where  $\omega$  is the angular frequency of input laser,  $\Delta\omega$  and  $\omega_{\text{FSR}}$  are the full width at half maximum (FWHM) and the free spectral range (FSR) of the filter in frequency domain, respectively,  $\omega_q = q\omega_{\text{FSR}}$  is the resonance angular frequency with the  $q$ -th longitudinal mode of the filter, and  $\rho$  is the maximum angular frequency deviation.  $K$  is the responsivity of PD,  $\alpha$  is defined as the relative misadjustment of the input laser frequency and the central frequency of the tunable FFP filter, and  $\beta$  is the modulation width which is related to the maximum angular fre-

\* This work has been supported by the National Natural Science Foundation of China (No. 60677024), the National High Technology Research Development Program of China (No. 2009AA03Z418), and the Educational Commission of Hubei Province of China (No.B20104401).

\*\* E-mail: qhbcs@yahoo.com.cn

frequency deviation  $\rho$  and FWHM of the filter.

Fig.1(a) illustrates the time response with the cavity length modulated by an AC signal in the cases of  $\alpha=0$ . It can be seen that one cyclical dither signal produces a detected signal at the frequency which is twice of the dither frequency. When the value of  $\beta$  is relatively small ( $\beta=0.2, 0.7$ ), the detected signal is weaker. However, the waveform of the detected signal can be seriously distorted when the value of  $\beta$  is relatively large ( $\beta=2$ ). Therefore, by judging whether the frequency of the detected signal is twice of dither frequency, we can determine whether the central wavelength of the filter is locked at the central wavelength of the laser. Meanwhile, the distortion with larger  $\beta$  further shows that the amplitude of AC signal should not be too large.

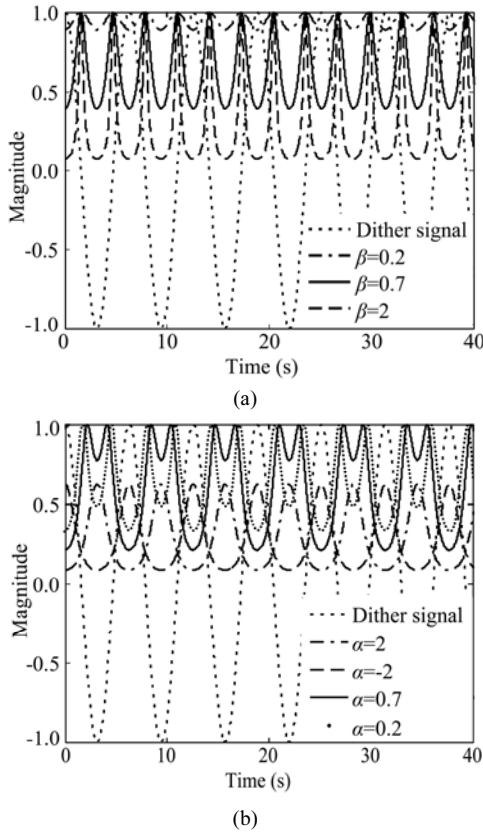


**Fig.1 Simulated time domain responses of PD signal at the situations of (a) no relative masadjustment  $\alpha=0$ , and (b) near zero relative masadjustment**

The case of the detected signal near  $\alpha=0$  is shown in Fig.1(b). When the relative misadjustment of the laser frequency and the filter frequency is relatively small ( $\alpha=0.2, 0.7$ ), the curve of the detected signal exhibits an approximately saddle-shaped dip. The phenomenon of smaller saddle point and narrower dip indicates a smaller relative masadjustment. When the value of  $\alpha$  is relatively large ( $\alpha=2, -2$ ), the curve of the detected signal exhibits a peak. It shows that the phase of the detected signal is the same as that of the dither signal when  $\alpha$  is positive, and the phase difference between the detected signal and the

dither signal is  $\pi$  when  $\alpha$  is negative. These simulation results can be utilized to calculate the relative masadjustment between the central wavelengths of the filter and the laser.

The relationship between the time difference  $\delta t$  and the relative frequency misadjustment  $\alpha$  is also considered quantitatively. From Eq.(1), suppose that the function  $f(t)$  is

$$f(t) = (\alpha + \beta \sin \omega_c t)^2. \quad (3)$$

The first-order and the second-order derivatives of  $f(t)$  are

$$f'(t) = 2\beta\omega_c(\alpha + \beta \sin \omega_c t) \cos \omega_c t, \quad (4)$$

$$f''(t) = 2\beta\omega_c^2(2\beta \cos 2\omega_c t - \alpha \sin \omega_c t). \quad (5)$$

As  $\beta$  is the modulation width which satisfies the condition of  $\beta>0$  and  $|\alpha|>|\beta|$ , the extreme value distribution of the FFP filter output can be described as follows.

(i) In the case of  $\alpha=0$ , which is corresponding to Fig.1(a), there is a minimum value of optical output as  $V_{Dmin}=KI_0/(1+4\beta^2)$  at  $\cos\omega_c t=0$ , and there is a maximum value as  $V_{Dmax}=KI_0$  at  $\sin\omega_c t=0$ .

(ii) In the case of relatively large  $\alpha$ , which is corresponding to Fig.1(b) ( $\alpha=2, -2$ ), there are two kinds of possibilities for the extreme output of the FFP filter. For  $\alpha>2\beta>0$ , there is a minimum value of optical output as  $V_{Dmin}=KI_0/(1+4\beta^2)$  at  $\sin\omega_c t=1$ , and there is a maximum value as  $V_{Dmax}=KI_0$  for  $\sin\omega_c t=-1$ . While for  $\alpha<-2\beta<0$ , there is a minimum value of optical output as  $V_{Dmin}=KI_0/(1+4\beta^2)$  at  $\sin\omega_c t=-1$ , and there is a maximum value as  $V_{Dmax}=KI_0$  at  $\sin\omega_c t=1$ .

(iii) In the case of relatively small  $\alpha$ , which is corresponding to Fig.1(b) ( $\alpha=0.2, 0.7$ ), there are also two kinds of possibilities. For  $0<\alpha<2\beta$ , there are a minimum value of optical output as  $V_{Dmin}=KI_0/(1+4\beta^2)$  at  $\sin\omega_c t=1$  and another minimum value as  $V_{Dmin2}=KI_0/(1+4(\alpha-\beta)^2)$  at  $\sin\omega_c t=-1$ , and there is a maximum value of optical output as  $V_{Dmax}=KI_0$  at  $\sin\omega_c t=-\alpha/\beta$ . For  $-2\beta<\alpha<0$ , the minimum value and maximum value of optical output are the same as those of the former ( $0<\alpha<2\beta$ ), but the difference of the corresponding time is exactly opposite.

Fig.2 illustrates the signal at the output of the tunable FFP filter clearly when the tunable FFP filter is modulated by an AC signal. It shows that one cycle of the driving signal produces a detected signal at the frequency which is twice of the dither frequency in the case of  $\alpha=0$ , where the central wavelength of the laser  $\lambda_1$  is equal to that of the filter. When the central wavelength of the laser  $\lambda_2$  is unequal to that of the filter, the detected signal exhibits an approximately saddle-shaped dip as shown in Fig.2.

The time difference  $\delta t$  between the peak of input signal and the trough of output optical signal is corresponding to the wavelength difference  $\Delta\lambda$ . As the output signal observed by a digital oscilloscope is the replica of the transmission spectral characteristic of the tunable FFP filter<sup>[13]</sup>, the difference between the central wavelength of

the laser and that of a transmission peak of the tunable FFP filter can be obtained by

$$\delta t : T = \Delta \lambda : FSR, \tag{6}$$

where  $T$  is the period of the input electrical signal.

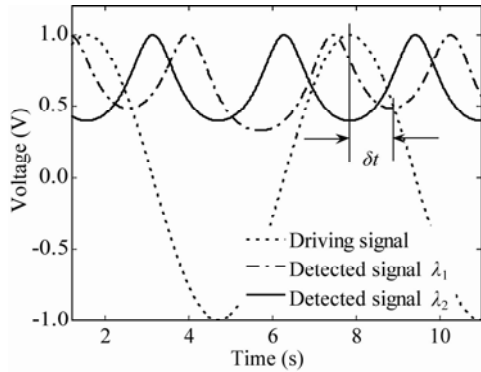


**Fig.2 Simulated dynamic responses for tunable FFP filter**

Based on Eqs.(2) and (6), a method for measuring the difference between the wavelength of the laser and that of the tunable FFP filter is proposed. The wavelength of the laser can be measured while the filter operates either in a closed-loop locking mode or in an opened-loop scanning mode.

The wavelength locking system of tunable FFP filter is shown in Fig.3. The source is a single-wavelength distributed feedback (DFB) laser diode with the central wavelength of 1551.37 nm. The  $FSR$  of the tunable FFP filter is 1.1 nm and its finesse is 12 at the test wavelength of 1550 nm. A function generator is used to supply an AC signal with amplitude of  $V_c$ . The optical output from the tunable FFP filter is detected by a PD and observed in a digital oscilloscope.

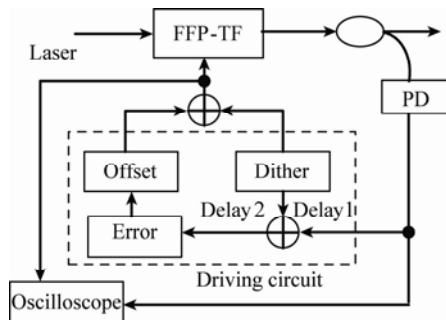
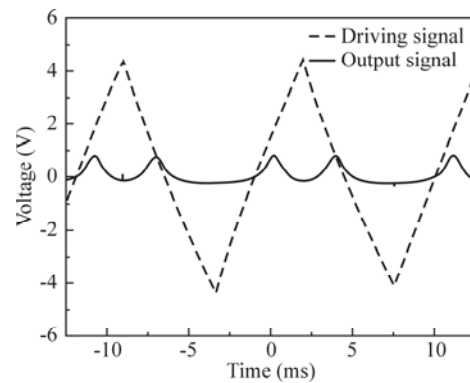


**Fig.3 Wavelength controller for scanning and locking modes**

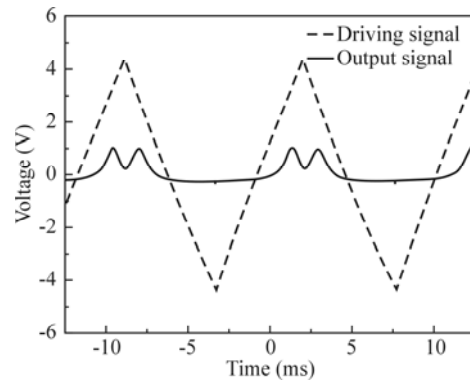
The driving circuit system consists of an opened-loop circuit and a closed-loop circuit. The intrinsic hysteresis of PZT element is defined as the time delay  $\tau_1$ , the time delay of power amplifier is defined as  $\tau_2$ , and then the total time delay ( $\tau_1 + \tau_2$ ) in the opened-loop circuit is delay1. The time constant  $\tau_3$  of low pass filter in the phase-locked-loop (PLL) is defined as delay2. As the

automatic voltage change applied on the FFP filter is decided by the error signal in the PLL system, delay2 should be less than delay1. Otherwise, it results in false feedback at the output of tunable FFP filter by the PLL.

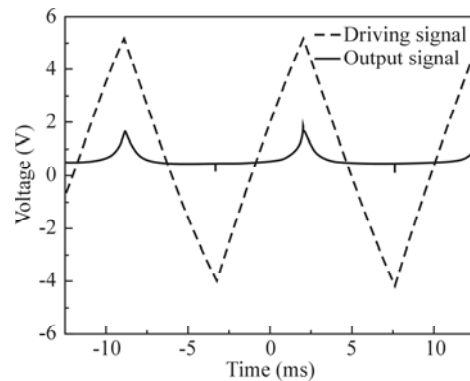
According to the requirements of time delays, a wavelength controller is designed, and the detected signals are shown in Fig.4 when the tunable FFP operates at the scanning mode. Fig.4(a) gives the measured trace at 1551.38 nm. The double-frequency of output signal in one cycle of the driving signal indicates that there is a small time delay between the input signal and the output signal. If the measured time delay for the opened-loop circuit is 0.030 ms, the difference between the central wavelength of filter and that of the laser is 0.13 nm.



(a) 1551.38 nm



(b) 1551.33 nm



(c) 1551.29 nm

**Fig.4 Measured detected signals at the scanning mode with different laser wavelengths**

Fig.4(b) gives the measured trace at 1551.33 nm. The measured time delay for the opened-loop circuit is 0.043 ms, and the difference between the central wavelength of filter and that of the laser is 0.19 nm. Fig.4(c) shows the measured trace at 1551.29 nm. The single frequency of optical output signal in one cycle of the driving signal implies that there is a large difference between the central wavelength of filter and that of the laser.

The measured wavelength difference between Fig.4(a) and Fig.4(b) is 0.06 nm. Meanwhile, the actual wavelength difference is 0.05 nm. Then the relative error between the measured wavelength and the actual wavelength is 0.01 nm. As the relative error is smaller than the wavelength resolution of the optical spectrum analyzer, which is 0.02 nm, it proves the validity of the wavelength measuring method.

In order to lock the central wavelength of filter at that of the laser, the detected signal needs to be mixed with a reference driving signal in a PLL circuit. Output signal from the PLL is either a positive or a negative direct current signal, which is used to adjust the bias current on the filter. Then the tunable FFP filter can be tuned by the polarity of the PLL output to the maximum transmission for tracking the central wavelength of the laser. The measured result of the tunable FFP filter for wavelength tracking and locking is shown in Fig.5. The mean voltage

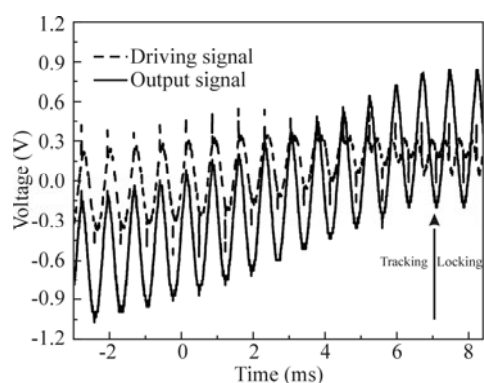


**Fig.5 Measured detected signal at the tracking and locking mode**

of the dither signal is adjusted by the PLL output signal, and an approximated double-peak emerges when the detected signal increases to a certain value. The total measuring time delay for the controller is 0.050 ms. As the time delay in the opened-loop circuit is 0.030 ms when there is a small time delay between the input signal and the output signal, the time delay in the closed-loop circuit is 0.020 ms. These results show that the difference between the central wavelength of filter and that of the laser is 0.25 nm, when the tunable FFP filter is locked at

the incident laser under the condition of short-time stability.

In summary, a high-precision wavelength controller for tunable FFP filter is presented, which is based on measuring the difference between the central wavelengths of the tunable FFP filter and the input laser. The measuring method is demonstrated through the dynamic simulation model of the tunable FFP filter experimentally, and the wavelength locking system of tunable FFP filter controller is designed by considering the time delays including the time delay of opened-loop circuit, the time constant of the closed-loop circuit and the intrinsic hysteresis of PZT element. The high-precision wavelength controller for tunable FFP filters is important for providing fast and stable alignment between the central wavelengths of the filter and a laser for optical communication and optical sensor applications.

## References

- [1] A. M. J. Koonen, *Wavelength Filters in Fiber Optics*, Springer Verlag, 271 (2006).
- [2] Y. Jiang, *Photonics Technology Letters* **20**, 75 (2008).
- [3] Yubin Ji, Shilie Zheng, Ze Li, Xiaofeng Jin, Xianmin Zhang and Hao Chi, *Microwave Opt. Technol. Lett.* **52**, 2090 (2010).
- [4] T. Takano, Y. Tomikawa, M. Aoyagi and C. Kusakabe, *Ultrasonics* **34**, 2 (1996).
- [5] JIA Zhen-an, LIU Jing, QIAO Xue-guang, WEI Ting, GAO Hong and FENG Hong-fei, *Journal of Optoelectronics · Laser* **22**, 649 (2011). (in Chinese)
- [6] J. A. Stone and A. Stejskal, *Proc. SPIE* **5190**, 327 (2003).
- [7] JIA Zhen-an, YING Xu-dong, QIAO Xue-guang and DING Feng, *Journal of Optoelectronics · Laser* **22**, 729 (2011). (in Chinese)
- [8] C. R. Locke, D. Stuart, E. N. Ivanov and A. N. Lutten, *Opt. Express* **24**, 21935 (2009).
- [9] H. Ding, X. Wu, J. Liang and X. Li, *Measurement* **42**, 1059 (2009).
- [10] K. Liu, W. C. Jing, G. D. Peng, J. Z. Zhang, D. G. Jia, H. X. Zhang and Y. M. Zhang, *Optics Communications* **281**, 3286 (2008).
- [11] Y. Jiang, *Applied Optics* **47**, 925 (2008).
- [12] K. Furutani and K. Iida, *Measurement Science & Technology* **17**, 2387 (2006).
- [13] L. L. Wang and T. Kowalczyk, *Photonics Technology Letters* **22**, 1267 (2010).
- [14] A. Agarwal, T. Banwell, P. Toliver and T. K. Woodward, *Photonics Technology Letters* **23**, 24 (2011).
- [15] M. Nakazawa, *Journal of Applied Physics* **59**, 2297 (1986).